PERGAMON

Deep-Sea Research I 45 (1998) 1515–1540

DEEP-SEA RESEARCH
PART I

# The sediments of Gunnerus Ridge and Kainan Maru Seamount (Indian sector of Southern Ocean)

R. Gersonde,[a,*] V. Spieß,[b] J.A. Flores,[c] R.A. Hagen,[d] G. Kuhn[a]

[a] *Alfred Wegener Institute for Polar and Marine Research, Postbox 120161, D-27515 Bremerhaven, Germany*
[b] *Fachbereich 5, Geowissenschaften, University Bremen, Postbox 330440, D-28334 Bremen*
[c] *Department of Geology, University of Salamanca, S-37008 Salamanca, Spain*
[d] *Naval Research Laboratory - Code 7420, 4555 Overlook Ave. SW, Washington, DC 20375*

Received 1 July 1997; accepted 16 December 1997

**Abstract**

Combined bathymetric, sediment echosounding and sediment coring data from two expeditions of the RV "Polarstern" (ANT-VIII/6, ANT-XI/4) provides the first more comprehensive overview of Cenozoic sedimentation in the remote area of the Gunnerus Ridge and Kainan Maru Seamount off the Antarctic Continent (Indian sector of Southern Ocean). The Neogene and Oligocene sediment sequences were affected by at least three generations of large scale slide and slump events, which occurred around the early/late Pliocene and the early/late Oligocene boundaries and during an earlier time period in the Paleogene. Possible triggers for slumping events might have been changes in the circulation pattern, changes in sea level, or earthquakes. Changes in water mass circulation could have affected the distribution of sediments since the onset of the Neogene in conjunction with the establishment of the Antarctic Circumpolar Current (ACC). The recovered sediments are predominantly biosiliceous mud and ooze, except for early Oligocene and Quaternary sequences, which contain calcareous nannofossils and foraminifera, respectively. The sediments have been deposited at low sedimentation rates ranging from a few millimeters to centimeters per 1000 yr. 

## 1. Introduction

The Gunnerus Ridge and the adjacent Kainan Maru Seamount are prominent bathymetric structures off the Antarctic Continent in the Indian sector of the

* Corresponding author. Fax: 0049 471 4831 149; e-mail: rgersonde@awi-bremerhaven.de

0967-0637/98/$ – see front matter 
PII: S0967-0637(98)00024-7

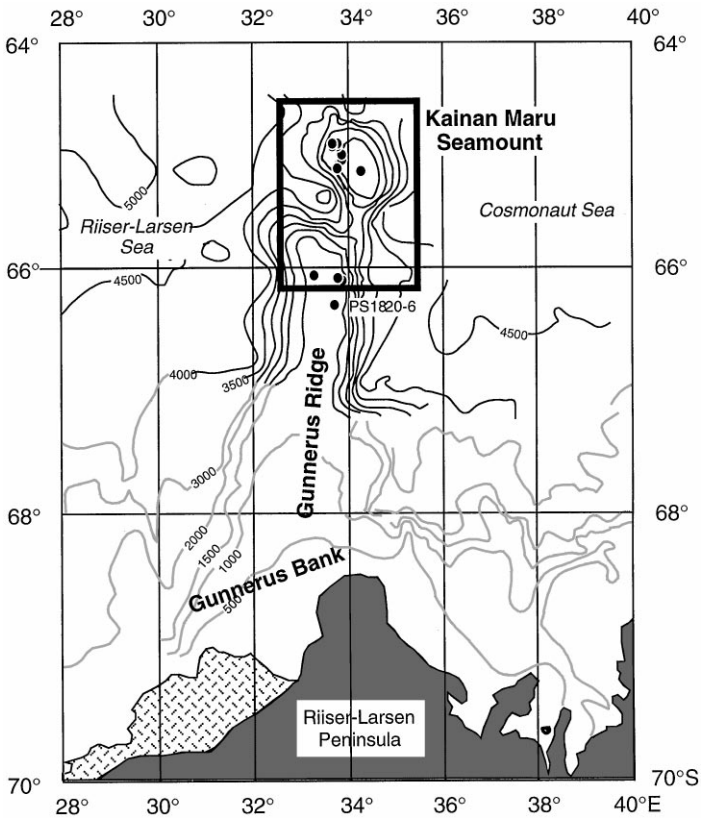


Fig. 1. Bathymetric map of Gunnerus Ridge and Kainan Maru Seamount (KMS) in the Indian Sector of the Southern Ocean, showing the sites of the recovered piston and gravity cores (contours in meters). Bathymetric data from Fütterer et al. (1991). Box indicates area of detailed KMS map (Fig. 2).

Southern Ocean. The Gunnerus Ridge extends ca. 200 km north from the Gunnerus Bank (off the Riiser-Larsen Peninsula) between 32° and 35°E into the Southern Ocean. It separates the deep-sea plains of the Riiser-Larsen Sea to the west and the Cosmonaut Sea to the east. The Gunnerus Ridge covers ca. 25,000 km$^2$; the minimum water depth over its flat crest increases from 1000 m in the south to ~1500 m in the north (Fig. 1). North of the Gunnerus Ridge is the Kainan Maru Seamount (KMS). The two features are separated by a steep and narrow EW-trending valley with water depth around 3200 m (Fig. 2).

The first geoscientific studies of the Gunnerus Ridge were conducted by Saki et al. (1987) and included a multichannel reflection seismic survey, sediment coring, and deep sea dredging. The seismic survey indicated that the Gunnerus Ridge consists of continental crust. Dredging in the valley between the Gunnerus Ridge and KMS recovered rocks of continental provenance, whereas no indications for a volcanic nature of the seamount were found. Only one core, recovering 2.5 m of foraminiferal

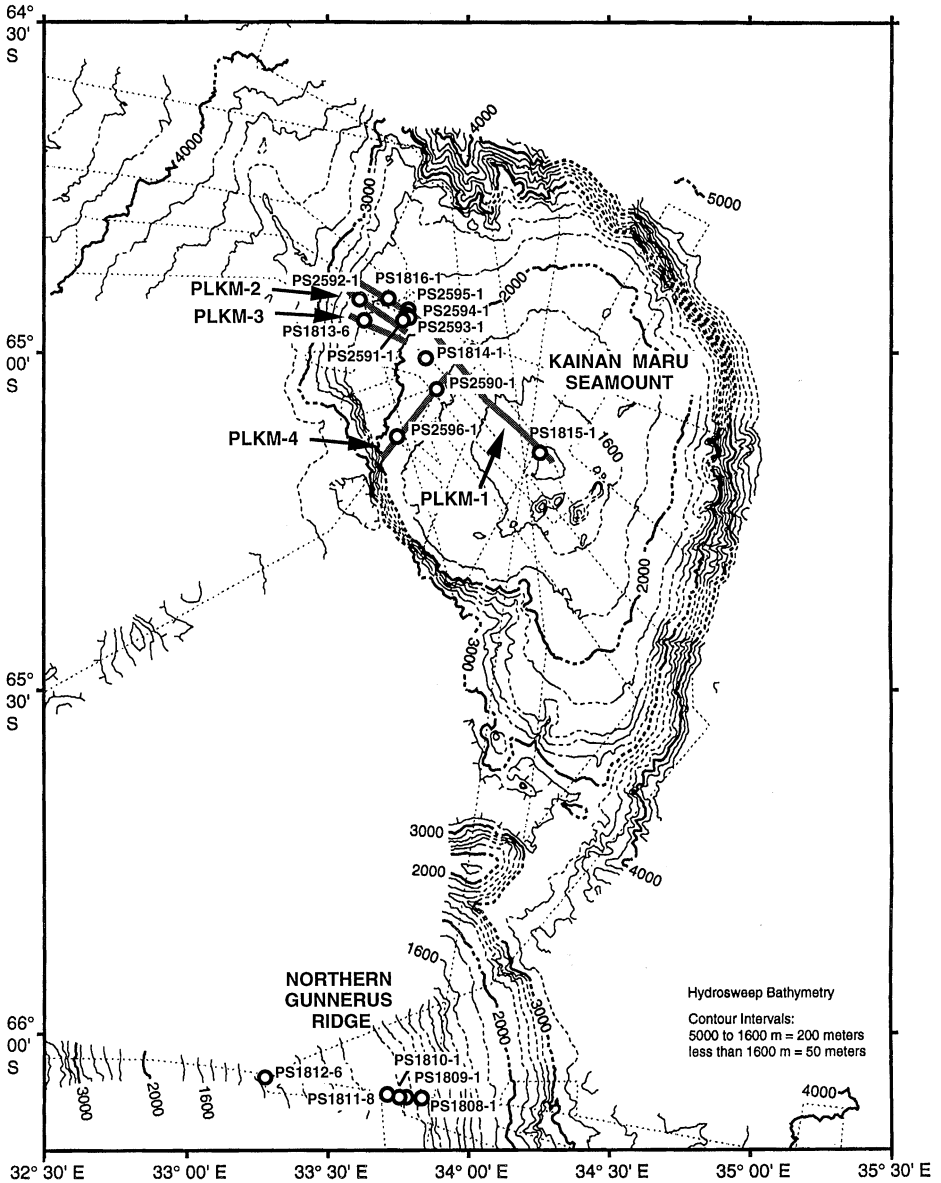


Fig. 2. Bathymetric map of Kainan Maru Seamount showing locations of piston cores and Parasound echosounding lines PLKM-1, PLKM-2, PLKM-3 and PLKM-4. Contour interval is 200 m; depths shallower than 1600 m are contoured at 50 m. Shiptracks of the Hydrosweep survey are shown as dashed lines.

ooze, apparently late Quaternary in age, was collected by the Japanese expedition on the Gunnerus Ridge at a water depth of 1309 m.

More comprehensive studies were accomplished during RV "Polarstern" expedition ANT-VII/6 in March–April of 1990 (Fütterer et al., 1991). These include a bathymetric survey with the Hydrosweep swath bathymetry system, high-resolution Parasound echosounding profiles, seismic multichannel and gravimetric surveys along and perpendicular to the crest of the Gunnerus Ridge and across KMS, and sediment sampling at various sites. This expedition represents the first geoscientific survey of KMS. The geophysical survey corroborates the Japanese results, showing that both Gunnerus Ridge and KMS are of continental nature and that both flanks are non-volcanic passive margins. Roeser et al. (1996) suggest that Gunnerus Ridge and KMS are a remnant of continental crust left behind when Madagascar and India separated from Antarctica through strike-slip motions. The seismic survey reveals that the Gunnerus Ridge is covered by sediments with a maximum thickness of ca. 250 m deposited on a fairly smooth basement topography. On KMS the sediment thickness is somewhat less (Roeser et al., 1996). Parasound echosounding profiles on the Gunnerus Ridge penetrated only to 20–40 mbsf (meters below sea-floor). Deeper penetration, up to 200 mbsf, was obtained on KMS and allowed the identification of distinct reflectors that can be correlated over larger distances in the seamount area (Spieß et al., in prep.). Large slide structures have been discovered using these echosounding profiles on the NW flank of KMS. The slides expose the failed surface, allowing coring of stratigraphically older sediments with conventional gravity and piston corers. These structures were resampled during expedition ANT-XI/4 from March to May 1994 (Kuhn, in press), and the bathymetric and Parasound surveys of KMS were expanded.

In this paper we present the first results of the geoscientific surveys conducted during ANT-VIII/6 and ANT-XI/4 on the Gunnerus Ridge and KMS, including bathymetric mapping, the echosounding survey and the stratigraphy of sediment cores collected at 17 sites. The cores record sediments spanning a time period between the Quaternary and the early Oligocene. Stratigraphic age assignment is based on diatom, silicoflagellate and nannofossil biostratigraphy that, in some cores, was combined with magnetostratigraphic data. This study provides a first overview of types, ages and sedimentation rates for sediments deposited on the Gunnerus Ridge and KMS. It can be used as a baseline for future piston core sampling providing a more continuous record of the Paleogene-Quaternary sediments deposited on KMS.

## 2. Material and methods

During RV "Polarstern" cruises ANT-VIII/6 and ANT-XI/4 the Parasound sediment echosounder system (STN Atlas Elektronik, Bremen), in combination with the digital data acquisition system ParaDigMA, was continuously operated to collect digital, ultra-high resolution seismic data. The hull-mounted Parasound system generates short signals of 2.5–5.5 kHz frequency within a narrow beam by use of the

parametric effect, which transfers energy from two high-frequency signals (here: 18 kHz and 20.5–23.5 kHz) to the difference frequency by non-linear interaction. The ParaDigMA system digitizes the seismograms at a 40 kHz sampling frequency and stores the data on magnetic tapes in SEGY format for further processing and replay. Heave, roll and pitch compensation significantly improve data quality and provide a vertical resolution on the order of 10 cm. A footprint size of only 7% of the water depth also provides superior lateral resolution compared to conventional 3.5 kHz echosounder systems.

The bathymetric survey was conducted with a Hydrosweep multibeam sonar system. Hydrosweep operates at a frequency of 15.5 kHz and generates acoustic signals that measure depths perpendicular to the ship's course with 59 2° pre-formed beams (Gutberlet and Schenke, 1989). In normal survey mode the beams are arranged in a 90° fan oriented athwartships, measuring a swath of seafloor with a width equal to 2 × the water depth. In shallow water (less than 2500 m) the total opening angle of this fan can be expanded to 120°, increasing the width of the surveyed swath to 3.7 × the water depth. Bathymetric data collected by the system are navigation corrected, edited to remove outliers and other errors and gridded using a gaussian weighted average scheme. The resulting gridded digital terrain model is contoured or used to create a variety of shaded-relief plots.

Hydrosweep data collected during RV"Polarstern" cruise ANT-VIII/6 on the Gunnerus Ridge consist of two long, parallel WNW–ESE lines, at about 66°S and 66.5°S. The lines extended from about 30°E to 39°E, providing profiles of the ridge. In addition, a long NNE–SSW line was collected along the crest of the ridge. The data are not complete enough to allow production of a good bathymetric map of the Gunnerus Ridge. Hydrosweep bathymetric data were collected on KMS during both RV"Polarstern" cruises ANT-VIII/6 and ANT-XI/4. Data coverage is about 70% on the summit of the seamount but does not extend far onto the seamount flanks except on the south and NE flanks. A contour map of the bathymetric data is shown in Fig. 2.

The 17 sediment cores were collected using gravity corer (GC) or piston corer (PC) devices (Table 1). Core descriptions are in the cruise reports by Fütterer et al. (1991) and Kuhn et al. (in press).

The diatom biostratigraphic zonation used to date the sediments is a combination of zones established by Gersonde and Burckle (1990), Baldauf and Barron (1991), Harwood and Mayurama (1992), and Gersonde and Bárcena (1998). The zonation extends over the last 35 Ma and is tied to the geomagnetic polarity record. Zonal age assignment and the age assignment of geomagnetic anomalies is based on the revised geomagnetic polarity time scale of Cande and Kent (1995) (Fig. 3). Diatom taxonomic references for the taxa identified from the sediment cores are in Akiba and Yanagisawa (1986), Baldauf and Barron (1991), Barron and Mahood (1993), Ciesielski (1983, 1986), Fenner (1978, 1984a, b, 1985), Gersonde and Burckle (1990), Gersonde (1990, 1991), Gombos (1977, 1983), Gombos and Ciesielski (1983), Harwood (1986, 1989), Harwood and Mayurama (1992), Schrader (1973, 1976), Schrader and Fenner (1976), Sheshukova-Poretzkaya (1962) and Yanagisawa and Akiba (1990). Diatom taxonomic revisions and description of new or yet inadequately known taxa are

Table 1
Core designation, coring instruments (GC = gravity corer, PC = piston corer), core length, core location, water depth based on corrected sound velocity, coring area (Gr = Gunnerus Ridge, KMS = Kainan Maru Seamount) and stratigraphic basal age of presented cores

| Core | Corer | Recovery (m) | Latitude | Longitude | Water depth (m) | Area | Basal age |
|---|---|---|---|---|---|---|---|
| PS1808-1 | GC | 0.78 | 66° 05.61′ S | 33° 49.85′ E | 1245 | GR | Late Pliocene |
| PS1809-1 | GC | 0.47 | 66° 05.48′ S | 33° 46.83′ E | 1188 | GR | ? Late Pliocene |
| PS1810-1 | GC | 0.5 | 66° 05.46′ S | 33° 45.21′ E | 1168 | GR | Mid Pliocene |
| PS1811-8 | GC | 2.76 | 66° 05.24′ S | 33° 42.67′ E | 1147 | GR | Early Pliocene |
| PS1812-6 | PC | 7.38 | 66° 03.76′ S | 33° 16.94′ E | 1356 | GR | Late Miocene (ca. 8.5 Ma) |
| PS1820-6 | GC | 1.76 | 66° 21.9′ S | 33° 46.8′ E | 1172 | GR | ? |
| PS1813-6 | PC | 12.54 | 64° 57.13′ S | 33° 38.03′ E | 2223 | KMS | Middle Miocene (ca. 13.7 Ma) |
| PS1814-1 | PC | 3.22 | 65° 00.54′ S | 33° 51.10′ E | 1964 | KMS | Quaternary |
| PS1815-1 | PC | 8.26 | 65° 09.03′ S | 34° 15.69′ E | 1526 | KMS | Early Pliocene (ca. 5 Ma) |
| PS1816-1 | PC | 10.02 | 64° 55.19′ S | 33° 42.86′ E | 2208 | KMS | Early Oligocene (ca. 30–29 Ma) |
| PS2590-1 | PC | 2.58 | 65° 03.30′ S | 33° 53.50′ E | 1861 | KMS | Quaternary |
| PS2591-1 | PC | 9.69 | 64° 57.10′ S | 33° 46.20′ E | 2053 | KMS | Middle Miocene (ca. 14.5 Ma) |
| PS2592-1 | PC | 8.61 | 64° 55.20′ S | 33° 37.00′ E | 2330 | KMS | Early Oligocene (ca. 30–28 Ma) |
| PS2593-1 | PC | 9.95 | 64° 56.90′ S | 33° 47.70′ E | 2040 | KMS | Middle Miocene (ca. 14 Ma) |
| PS2594-1 | PC | 11.38 | 64° 56.80′ S | 33° 47.40′ E | 2047 | KMS | Early early Miocene-late Oligocene |
| PS2595-1 | PC | 9.54 | 64° 56.08′ S | 33° 47.20′ E | 2059 | KMS | Early Oligocene (ca. 31–30 Ma) |
| PS2596-1 | PC | 5.81 | 65° 07.60′ S | 33° 45.20′ E | 1880 | KMS | Quaternary |

beyond the scope of this paper and will be published elsewere. This includes the transfer of Miocene taxa belonging to the genus *Nitzschia* to the reinstated genus *Fragilariopsis*, as discussed in Gersonde and Bárcena (1998). Taxa such as *Thalassiosira* sp. 1 from Fenner (1978) and *Hemiaulus* sp. A from Harwood (1986), of which both might have biostratigraphic significance for Paleogene southern high-latitude zonations, will be described in detail in a separate paper. The same is true for *Coscinodiscus lewisianus* and related forms, which should be removed from the genus *Coscinodiscus*. The zonal assignment of the early Oligocene *Rhizosolenia oligocenica* Zone was tentatively changed into the *R. gravida/oligocenica* Zone because of apparent taxonomic uncertainities. The zone originally described by Gombos and Ciesielski (1983) as *R. gravida* Zone was renamed by Harwood et al. (1989), following the taxonomic consideration of Fenner (1985) that *R. gravida* is conspecific with *R. oligocenica*. Considering the original descriptions and the photographic

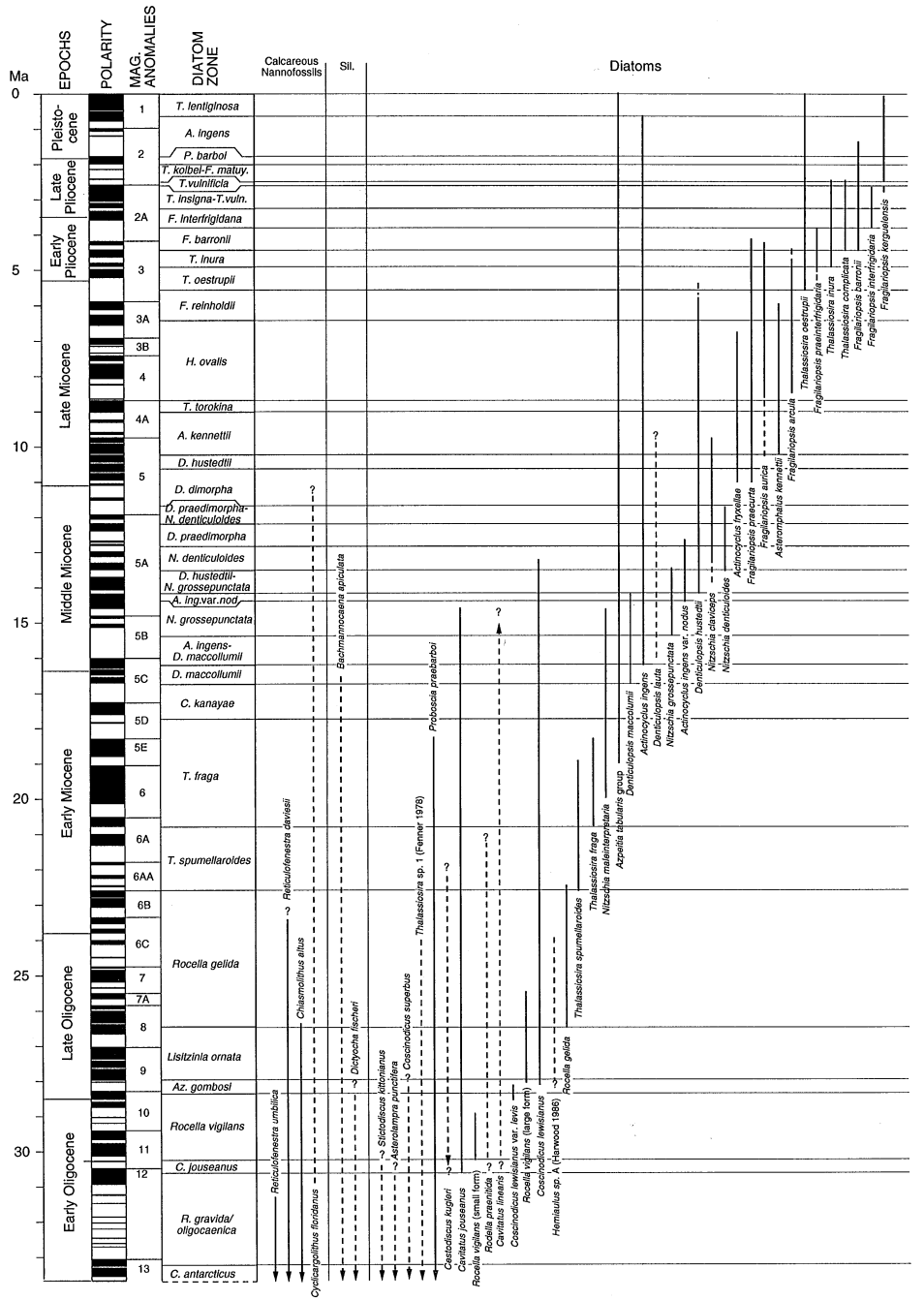


Fig. 3. Diatom zonation and age ranges of diatom, silicoflagellate and calcarous nannofossil taxa used for stratigraphic age assignment correlated with the geomagnetic polarity record from Cande and Kent (1995). Dashed lines indicate trace or uncertain occurrence range of taxa.

documentation of *R. gravida* by Gombos and Ciesileski (1983) and of *R. oligocenica* by Schrader (1976), which indicate distinct differences in shape and structure between these taxa, it appears difficult to justify combining both as suggested by Fenner (1985). Accurate morphological investigations need to be made to resolve this problem.

Silicoflagellate stratigraphy is according to McCartney and Wise (1990) and Perch-Nielsen (1985a). The calcareous nannofossil age assignment relies on Berggren et al. (1995), Perch-Nielsen (1985b), Wei and Wise (1990, 1992) and Young et al. (1994). The diatom zonation and the stratigraphic species ranges of diatom, silicoflagellate and calcareous nonnofossil taxa used for stratigraphic age assignment are shown in Fig. 3.

Geomagnetic measurements are available from three cores (PS1812-6, PS1813-6, PS1816-1), allowing the establishment of detailed age-depth models and sedimentation rates for selected Quaternary, Pliocene, and late and middle Miocene time periods. The piston cores were sampled at a 5 cm spacing for paleomagnetic analyses. Between measurements of the magnetization vector, which were carried out with a 3-axis cryogenic magnetometer (Cryogenic Consultants, Inc.) at the University of Bremen, all cubic samples (6 $cm^3$ volume) were subjected to successively increasing alternating fields of up to 80 mT strength. The characteristic remanent magnetization of each sample was determined by averaging individual magnetization vectors for those demagnetization steps, where the mean direction coincides with the average of the difference vectors. Because of the steep inclination values, polarities were derived directly from their sign.

## 3. Results

### *3.1. Kainan Maru Seamount*

The Kainan Maru Seamount (KMS) is about 60 km wide and 120 km long, with the long axis of the seamount oriented NNW–SSE (Fig. 2). The gap between the seamount and Gunnerus Ridge to the south is about 30 km wide and about 1200 m deep. It forms a saddle, connecting the seamount and the ridge and separating the basins to the east and west. The summit area of the seamount is gently-domed, rising from about 2000 m at the break in slope to less than 1500 m at its center. In the south central part of the seamount summit occur dome-like structures with diameters of a few kilometers that rise ca. 100–150 m above the basement. The presence of these structures, which are not covered by sediment, apparently caused strong winnowing and the formation of narrow moats between the domed structures and the surrounding sediment deposits.

The eastern flank of the seamount is steep (slopes over 30°), dropping rapidly from 2400 to 5000 m, and is cut by numerous small erosional channels. The western flank of the seamount drops steeply from 2000 to 3000 m but then slopes gently (less than 2°) down to the west. The northwestern and southern flanks of the seamount do not show the steep section seen on the western flank but slope gently (3° to 5°) from the summit to the adjacent seafloor. This asymmetry in the seamount's flanks is very distinct.

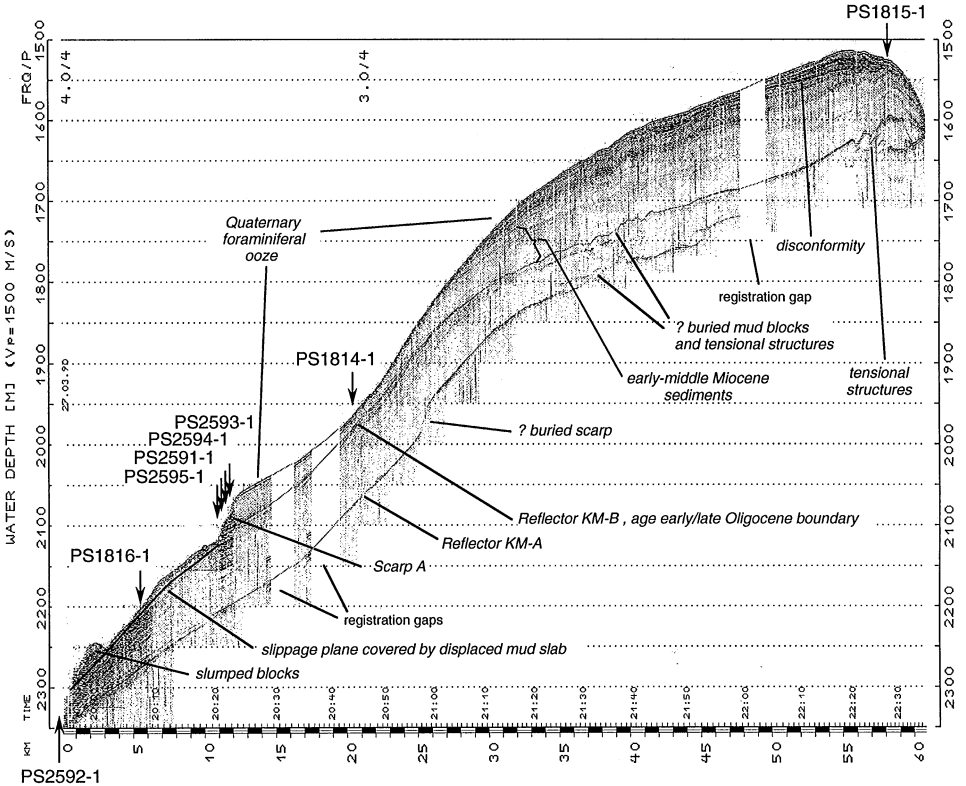


Fig. 4. Parasound-echosounding line PLKM-1 on the NW flank of Kainan Maru Seamount (for location see Fig. 2) showing Reflectors KM-A and KM-B, slippage planes and scarps. Cores were not recovered exactly on Line KM-1, thus water depth at core locality (Table 1) may not coincide with depth on profile. Differences in water depth may also arise because depth on Parasound profile is calculated with 1500 m/s sound velocity while core depth represents corrected water depth.

Depths of over 5000 m are reached within 40 km of the summit to the east, whereas one must travel over 100 km west to reach similar depths. The northwestern flank of the seamount proper may actually be as steep as the eastern flank but appears to be buried by a thick apron of sediment.

Eleven sediment cores are available from KMS. They all were recovered from the gently sloping northwestern flank of KMS, where sediments reach a total thickness of more than 200 m (Figs. 2 and 4, Table 1). Acoustically these sediments can be subdivided into well layered sediment packages separated by distinct reflectors, which we have named KM-A and KM-B. These reflectors represent discontinuities in the sediment record, as documented by Parasound-echosounding lines PLKM-1, PLKM-2, PLKM-3 and PLKM-4 from the western flank of KMS (Figs. 2 and 4–7). In the region of the seamount summit Reflector KM-B shows down-slope tensional structures (Fig. 4). The surface morphology of these tensional structures is transferred into

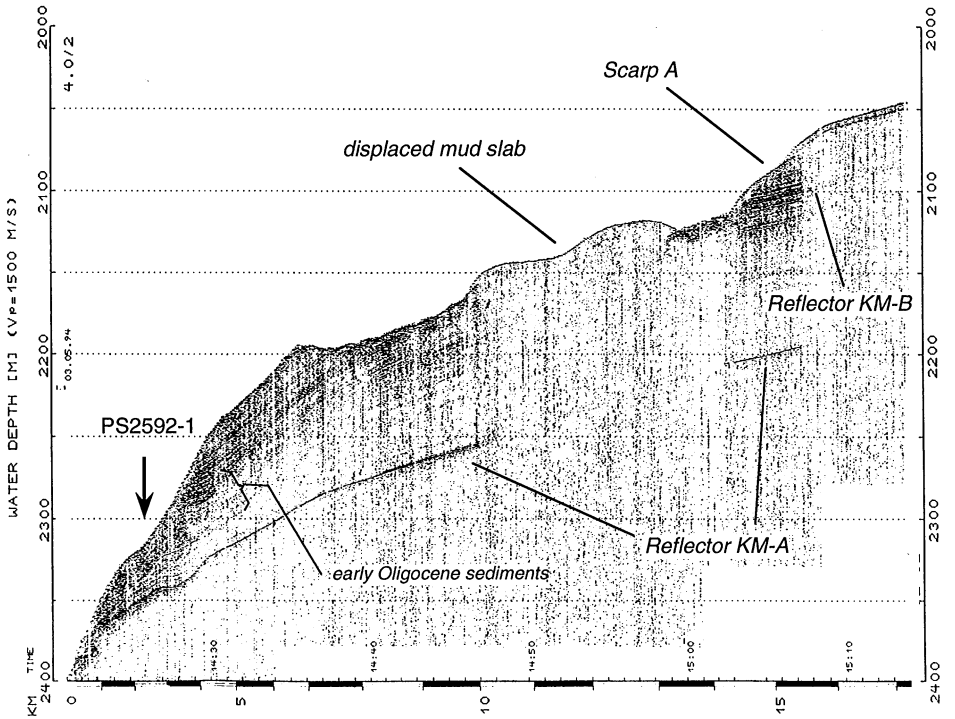


Fig. 5. Parasound-echosounding line PLKM-2 on the lower NW flank of Kainan Maru Seamount (for location see Fig. 2) showing Reflectors KM-A and KM-B, a slippage plane and Scarp A. Core PS2592-1 was not recovered exactly on Line PLKM-2. Differences in water depth may also arise because depth on Parasound profile is calculated with 1500 m/s sound velocity while core depth represents corrected water depth.

the overlying sediment structure. Between 1700 and 1800 m water depths KM-A and KM-B are irregular and wavy, becoming smoother towards the lower flank of KMS (Fig. 4). We interpret these structures to represent the surface of dislocated sediment blocks buried by younger sediments and probable tensional structures. Between 1900 and 2000 m water depths the sediments above KM-B are highly thinned (Fig. 4), a pattern that was also observed in the area southwest of PLKM-1 at the same water depth, as recorded on PLKM-3 and PLKM-4 (Figs. 6 and 7). These features indicate that KM-A and KM-B are linked with large sediment slides, which affect the sediment deposition pattern of the entire western flank of KMS. Linked to the slides are sediment detachment events, which produce scarps, as seen at water depths around 2075–2100 m on PLKM-1 and PLKM-2 (Scarp A on Figs. 4 and 5). Scarp A, which formed above KM-B, is about 60 m high and exposes a submarine outcrop of the sediments deposited above KM-B. In order to sample these sediments a suite of four cores (PS2591-1, PS2593-1, PS2594-1, PS2595-1) was recovered at Scarp A at different water depths. The slippage plane below the scarp is covered by dislocated sediment

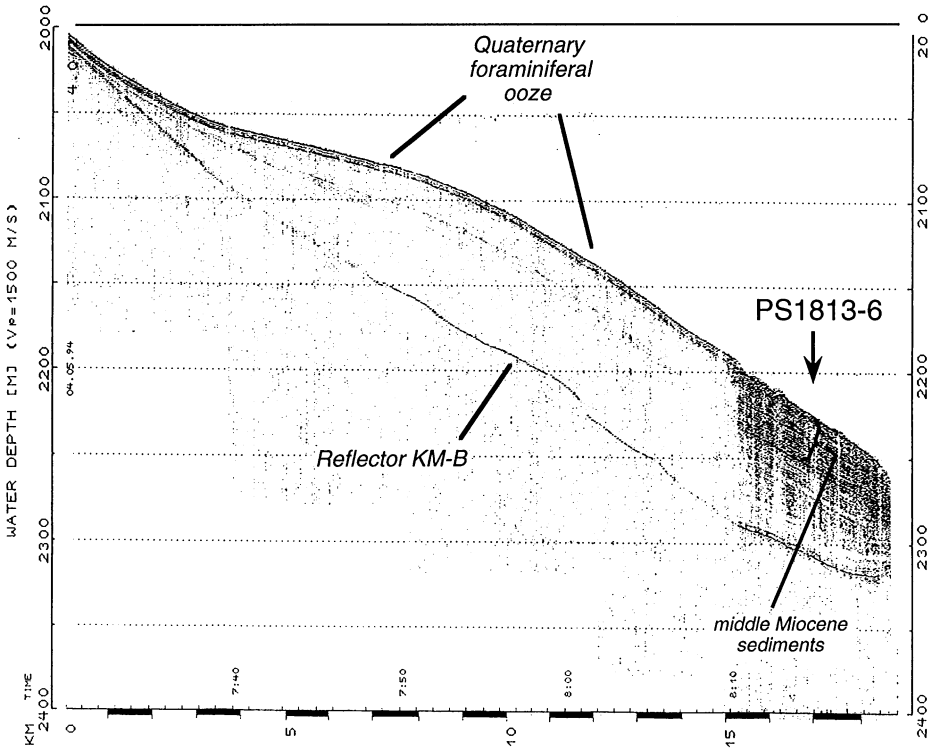


Fig. 6. Parasound-echosounding line PLKM-3 on the lower NW flank of Kainan Maru Seamount (for location see Fig. 2) showing thinning of sediments above Reflector KM-B at around 2000 m depth. This area southwest of PLKM-1 and PLKM-2 is not affected by a sediment detachment event as shown on Figs. 4 and 5. Core PS1813-6 was not recovered exactly on Line PLKM-3. Differences in water depth may also arise because depth on Parasound profile is calculated with 1500 m/s sound velocity while core depth represents corrected water depth.

blocks and sheets. A buried scarp is possibly seen at around 1975 m below the sea surface on Reflector KM-A. A third distinct disconformity observed in the sediment sequence deposited on the summit of KMS cannot clearly be linked with a sediment slide. Most sediment cores were collected at sites on or close to PLKM-1 in order to sample the different types and ages of sediment deposited on KMS and to date the event that produced Scarp A and the KM reflectors.

Core PS1815-1 (core length 8.26 m, water depth 1525 m) is the shallowest core recovered from the thick pile of sediments deposited on the summit of KMS and is located on the southeastern end of Parasound line PLKM-1 (Fig. 4). At its base the core consists of diatomaceous mud associated with the upper portion of the early Pilocene *T. oestrupii* Zone, based on the occurrence of the nominate species together with *Fragilariopsis aurica*, *F. praecurta* and *F. praeinterfrigidaria* (Fig. 3). This is followed by a diatom ooze characterized by assemblages of the *Thalassiosira inura* Zone. A disconformity separates the lower early Pliocene from diatom bearing

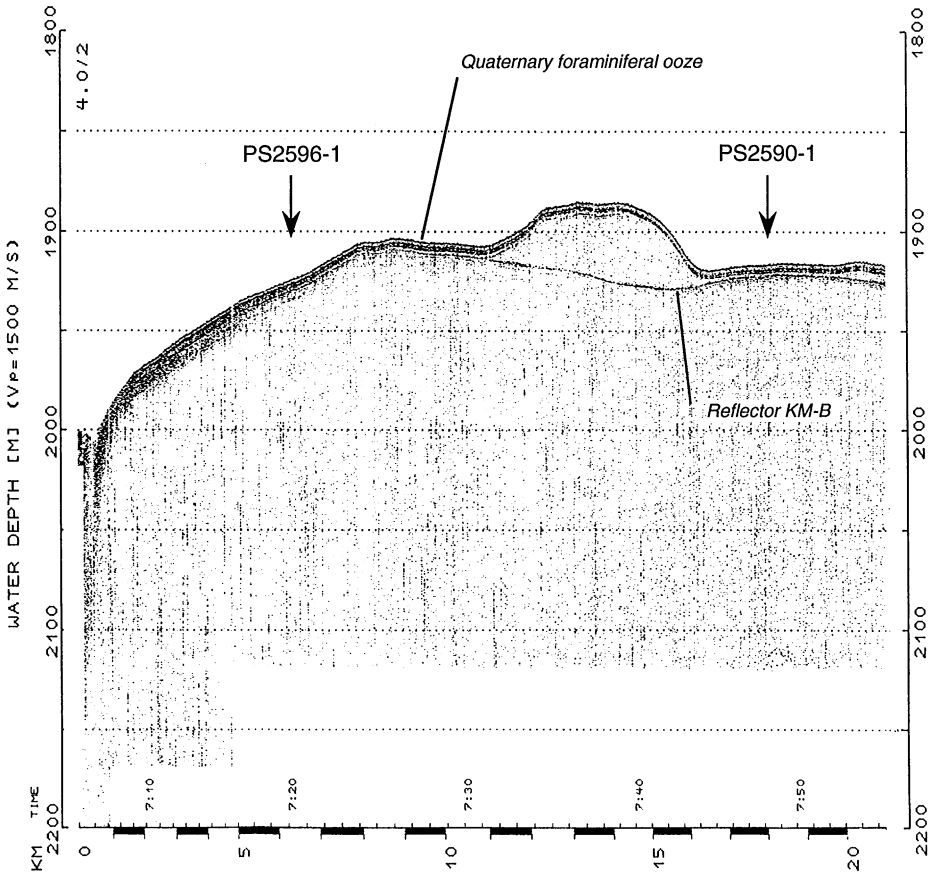


Fig. 7. Parasound-echosounding line PLKM-4 on the western flank of Kainan Maru Seamount (for location see Fig. 2) at water depths around 1900 m showing thin sediment cover above Reflector KM-B. Strong reflectors mark Quaternary foraminiferal ooze. Differences in water depth may also arise because depth on Parasound profile is calculated with 1500 m/s sound velocity while core depth represents corrected water depth.

foraminiferal muds deposited in the early late Pliocene. Poor preservation of the diatom assemblages prevents detailed age assignment. This is also true for the top three meters of PS1815-1, which are a foraminiferal ooze. Trace occurrences of *Fragilariopsis kerguelensis* and *Actinocyclus ingens* indicate a late Pliocene-Quaternary age (Fig. 8).

Cores PS1814-1 (core length 3.22 m, water depth 1964 m), PS2590-1 (core length 2.58 m, water depth 1861 m) and PS2596-1 length 5.81 m, water depth 1880 m) were all located where the sediments above Reflector KM-B were highly thinned (Figs. 4 and 7) in order to sample older sediments below KM-B. PS1814-1 was recovered very close to PLKM-1. The other two cores were collected in a similar seismic environment southwest of PLKM-1 on Parasound line PLKM-4 (Fig. 7). All cores did not

penetrate deeper than 6 m into the sediment, because of the presence of sandy foraminiferal ooze or mud at the surface. This layer forms a strong seismic bottom reflector and prevented deeper penetration. The longest of the three cores, PS2596-1, penetrated sandy glauconitic sediments, possibly related to Reflector KM-1B. At 4.5 m core depths this is overlain by foraminiferal mud and ooze. The sediment contains only poorly preserved diatoms with trace occurrences of *Fragilariopsis kerguelensis* and *Actinocyclus ingens* and thus are similar to those sampled in the upper portion of PS1815-1. This is also true for PS2590-1 and PS1814-1. Both cores recovered only late Pliocene – Quaternary foraminferal ooze, which covers the top and upper flanks of KMS and Gunnerus Ridge.

Core PS2593-1 (core length 9.95 m, water depth 2040 m) is the shallowest of the suite of four cores over a depth range of 19 m recovered at slide Scarp A on PLKM-1 (Fig. 4). It consists of diatom ooze, except for the upper ca. 1.9 m, which is diatomaceous mud topped by a veneer of foraminiferal ooze. The diatom ooze is in the middle Miocene *Denticulopsis hustedii-Nitzschia grossepunctata* Zone as indicated by the occurrence of the nominate species together with taxa such as *Actinocyclus ingens*, *A. ingens* var. *nodus*, *Denticulopsis lauta*, *Nitzschia claviceps* and *N. januaria*, in the absence of *N. denticuloides* (Fig. 3). The overlying diatomaceous mud ranges in the middle Pliocene *Fragilariopsis interfrigidaria* Zone and is separated from the diatom ooze by a disconformity. The recovered diatom assemblages are characterized by *A. ingens*, *Fragilariopsis barronii*, *F. interfrigidaria*, *Thalassiosira inura* and *Rouxia isopolica* (Fig. 8).

Core PS2594-1 (core length 11.38 m, water depth 2047 m) is strongly disturbed in its lowermost meter, as indicated by mixed Miocene diatom assemblages overlain by stratigraphically older sediments. The oldest sediments are at ca. 10.4 m core depth and can be placed in the Oligocene to early Miocene based on the co-occurrence of *Asteromphalus symmetricus*, *Cavitatus linearis*, *C. jouseanus*, *Azpeitia oligocaenica* and *Cestodiscus kugleri* in the absence of *Denticulopsis* spp. and *Actinocyclus ingens*. Poor preservation of the assemblages and the lack of distinct age-indicative taxa prevents a detailed age assignment of the sediments. A disconformity occurs at around 9 m, followed by diatomaceous mud deposited in the middle Miocene *Nitzschia grossepunctata* Zone. In addition to the nominate species, *Actinocyclus ingens*, *Coscinodiscus lewisianus*, *Denticulopsis lauta* and *D. maccollumii* also occur. Around 7.8 m is the first occurrence of *Actinocyclus ingens* var. *nodus*, followed at around 6 m by the first occurrence of *Denticulopsis hustedtii*. In this section the sediments grade into diatom ooze. The absence of *Nitzschia denticuloides* in the diatom ooze that continues up to ca. 0.8 m indicates a middle Miocene age for this interval (*D. hustedtii–N. grossepunctata* Zone). The top of the core consists of diatom-bearing mud that was deposited during the later part of the middle Pliocene *Fragilariopsis interfrigidaria* Zone; this is covered by a centimeters thick foraminiferal ooze (Fig. 8).

Core PS2591-1 (core length 9.69 m, water depth 2053 m) sampled a section that compares well with the middle Miocene section recovered in PS2593-1 and PS2594-1. The base of the core is in diatomaceous mud of the upper *Nitzschia grossepunctata* Zone followed by diatomaceous ooze that can be placed in the *A. ingens* var. *nodus*

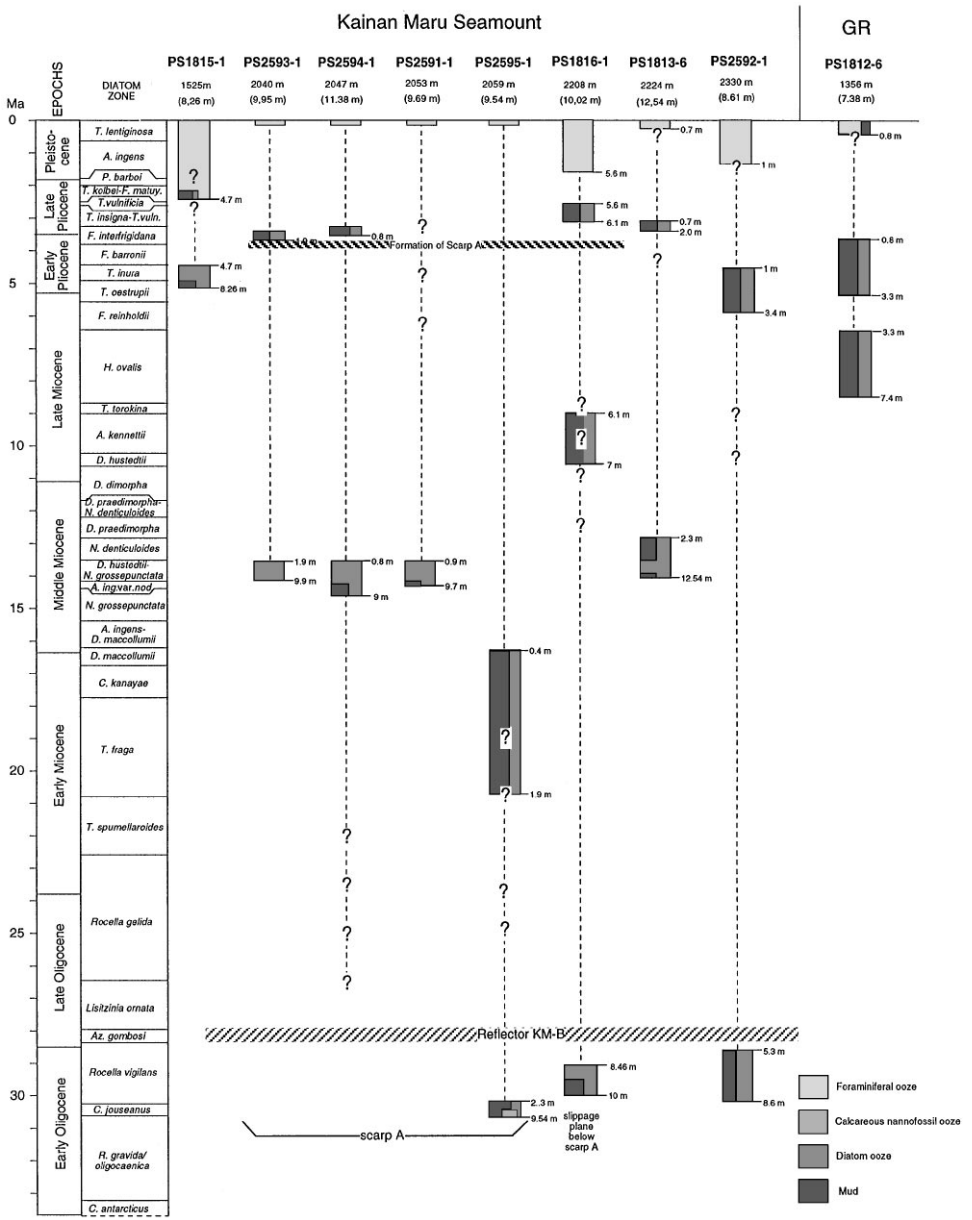


Fig. 8. Schematic representation of stratigraphic ranges of sediment cores and core sections, correlated with Quaternary-Oligocene diatom biostratigraphic zones, and general core lithology. Meters in core log columns indicate core depth of sections.

and the *D. hustedtii-N. grossepunctata* Zone. The upper 0.9 m consists of diatom ooze and mud with mixed Miocene and Pliocene diatom assemblages, covered by a thin layer of foraminiferal ooze (Fig. 8).

Core PS2595-1 (core length 9.54 m, water depth 2059 m) is the deepest of the suite of four cores from slide Scarp A. The lower portion of the core consists of diatom-bearing nannofossil mud, which grades into diatom-bearing mud at around 7 m core depth. The nannofossil assemblages are dominated by *Reticulofenestra daviesii* and *Chasmolithus altus*. Both taxa are long-ranging in southern high-latitudes, having their first occurrence in the Eocene and their last occurrence in the early Miocene and late Oligocene, respectively (Wei and Wise, 1990) (Fig. 3). Sporadic records of the Oligocene *Cyclicargolithus floridanus* were encountered in the upper portion of the calcareous interval. In the absence of *Reticulofenestra umbilica*, a taxon that has its last occurrence at the base of the *Chiasmolithus altus* Zone (Wise, 1983) in the middle early Oligocene (Fig. 3), we interpret the nannofossil assemblages to indicate a late early Oligocene to late Oligocene age in the *C. altus* Zone. This is corroborated by the co-occurrence of *Cavitatus jouseanus* and *C. linearis*, both diatom taxa that have their first occurrence in the late early Oligocene (Fig. 3). *Cavitatus jouseanus*, which ranges into the early middle Miocene *Nitzschia grossepunctata* Zone, was encountered from the base of the core upto around 0.4 m core depth. Taxa such as *Stictodiscus kittonianus*, *Asterolampra punctifera*, *Thalassiosira* sp. 1 (Fenner 1978), *Hemiaulus* sp. A (Harwood 1986), *Cestodicus kugleri*, *Rocella praenitida* and *Coscinodiscus superbus* point to an early Oligocene age for the core interval between the core base and ca. 2.3 m core depth. Considering the calcareous nannofossil ranges and the absence of *Rocella vigilans*, an age corresponding with the *Cavitatus jouseanus* Zone can be inferred. This interpretation implies that the range of the yet poorly known *Hemiaulus* sp. A (Harwood 1986) should be expanded into the early Oligocene (Fig. 3). Between 2.3 and 1.9 m is a zone with unclear age assignment in the late Oligocene to early Miocene. From 1.9 and 1 m core depth occur *Thalassiosira fraga* and *T. spumellaroides*, followed up to 0.7 m by assemblages consisting of few to common occurrences of *Denticulopsis maccolumii* together with rare *Azpeitia tabularis* and *Nitzschia maleinterpretaria*. This indicates an age corresponding with the *T. fraga* Zone and the *D. maccollumii* Zone in the early Miocene. Between 0.7 and 0.4 m occurrences of Miocene and Pliocene diatoms indicate a zone of mixed and disturbed sediments, which are topped by diatom-bearing foraminiferal mud with Quaternary diatoms.

Core PS1816-1 (core length 10.02 m, water depth 2208 m) sampled a slab of dislocated sediment deposited on the slippage plane below slide Scarp A as recorded by nearby PLKM-1 (Fig. 4). It consists of diatomaceous mud and diatom ooze between the base of the core and 8.46 m (Fig. 9). This section can be placed into the late early Oligocene *Rocella vigilans* Zone because of the co-occurrence of *Rocella vigilans* (small forms), *Caviatus jouseanus*, *C. linearis*, *C. rectus*, *Cestodiscus kugleri* and *Hemiaulus* spp. in the absence of *Lisizina ornata* and *Rocella gelida* (Fig. 3). Other taxa occurring in this section are *Asteromphalus symmetricus*, *Coscinodiscus superbus*, *Hemiaulus* spp., *Kisseleviella carina*, *Pseudotriceratium chenevieri*, *Stephanopyxis* spp. and the silicoflagellate *Dictyocha fischeri*. This sediment interval is marked by a change from normal to reversed geomagnetic polarity. The normal interval is

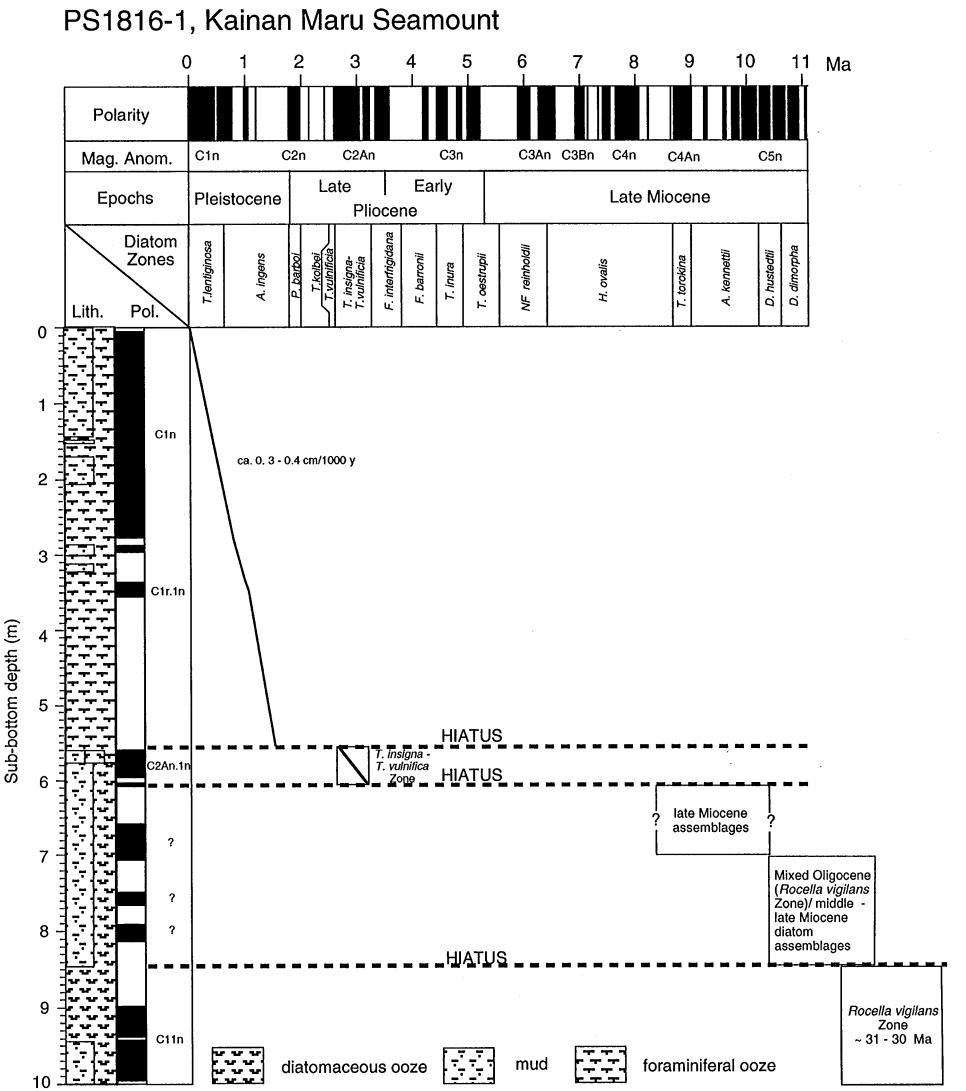


Fig. 9. Age-depth model for Core PS1816-1, based on combined diatom and geomagnetic polarity stratigraphy. Age assignment of geomagnetic polarities according to Cande and Kent (1995).

interpreted to represent a portion of C11n, correlated with the lower *Rocella vigilans* Zone (Fig. 3). Similar strata have been sampled in Core PS2592-1, located nearby. Above a disconformity marked by a sharp lithologic change (8.46 m) occurs a diatom mud including a mixture of early Oligocene and middle–late Miocene diatom assemblages. The less steep geomagnetic inclinations indicate disturbance of sediments by slumping and mixing of sediments of different ages. Above 7 m are diatom muds that

seem to be undisturbed by mixing. They bear assemblages characterized by common occurrences of *Denticulopsis hustedtii*. Co-occuring species are *Actinocyclus fryxellae*, *Asteromphalus kennettii*, *Fragilariopsis arcula* and *F. aurica*, which indicate a late Miocene sediment age that falls into a time period covered by the *Denticulopsis hustedtii* and the *Asteromphalus kennettii* Zones (Fig. 3). Another disconformity at around 6.1 m separates the late Miocene from a thin middle Pliocene interval, which is placed into the *Thalassiosira insigna–T. vulnifica* Zone based on the occurrence of the nominate species together with *Fragilariopsis barronii*, *F. interfrigidaria*, *Thalassiosira inura* and *T. complicata*. The foraminiferal mud and foraminiferal ooze, which contain up to 75% carbonate above this section, bear only rare and trace diatom occurrences. The foraminiferal sediments are separated from the underlying middle Pliocene sediments by a disconformity at around 5.6 m and have been deposited during the last 1.5–1.8 Ma, thus at an average sedimentation rate of ca. 0.3–0.4 cm per 1000 yr, based on the interpretation of the geomagnetic data obtained from this interval (Fig. 9).

Core PS1813-6 (core length 12.54 m, water depth 2224 m) was collected west of the Scarp A area from sediments that were not affected by the detachment event that produced the scarp, as recorded on PLKM-3 (Fig. 6). The core sampled sediment sequences similar to those obtained at the scarp in cores PS2591-1, PS2593-1 and PS2994-1 (Fig. 8). The base of PS1813-6 is in the diatomaceous mud of the lowermost *Denticulopsis hustedtii–Nitzschia grossepunctata* Zone (middle Miocene) (Fig. 10). This is indicated by the presence of the nominate species. Other stratigraphically important taxa are *Actinocyclus ingens* var. *nodus* and *Nitzschia claviceps*. At around 5.1 m is the base of the *Nitzscgua denticuloides* Zone, indicated by the first occurrence of the nominate species. The middle Miocene sequence is bounded by a disconformity at around 2.3 m. It is overlain by diatomaceous mud that bears a mixture of diatoms ranging in the early Pliocene and a section assigned to the early late Pliocene *Thalassiosira insigna–T. vulnifica* Zone and the *Fragilariopsis interfrigidaria* Zone. Above another disconformity at 0.7 m occurs late Quaternary foraminiferal ooze (carbonate content 50–60%) that contains only a few diatoms. Based on a combined magnetostratigraphic and biostratigraphic age/depth model, the middle Miocene diatomaceous mud and diatom ooze were deposited at rates around 1.5 cm/1000 yr (*D. hustedtii–N. grossepunctata* Zone) and 0.4 cm/1000 yr (*Nitzschia denticuloides* Zone) (Fig. 10).

Core PS2592-1 (core length 8.61, water depth 2330 m) is the deepest core on the northwestern flank of KMS, collected just above the steep flank below 2400 m as recorded on PLKM-2. The core sampled a section consisting of diatomaceous ooze in the lowest meter of the core, grading into diatomaceous mud and diatom-bearing mud that is topped by a 1 m-thick foraminiferal ooze. The basal diatom ooze can be placed into the late early Oligocene *Rocella vigilans* Zone. The assemblages compare well with those from the same time interval collected in PS1816-1. The overlying diatomaceous mud and diatom-bearing mud contain only moderate to poorly preserved diatom assemblages. Prominent taxa are *Caviatus jouseanus*, *C. linearis* and *C. rectus*, all ranging from the late early Oligocene into the early Miocene, as well as *Hemiaulus* spp., *Stephanopyxis* spp. and *Trinacria excavata*. The presence of *Coscinodiscus*

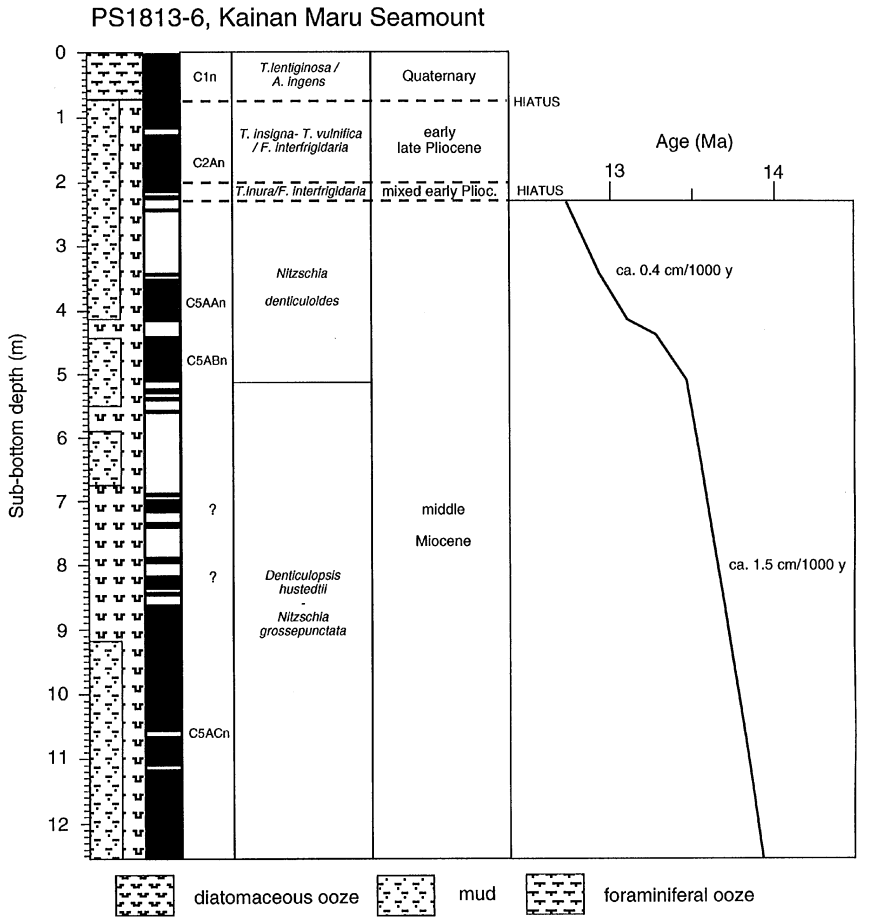


Fig. 10. Combined diatom and geomagnetic polarity stratigraphy of core PS1813-6, including an age-depth model for the middle Miocene core section. Age assignment of geomagnetic polarities according to Cande and Kent (1995).

*lewisianus* var. *levis*, *C. lewisianus* and the silicoflagellate *Dictyocha fischeri* between 7 and 5.3 m core depths indicates an age close to the early/late Oligocene boundary (Fig. 3). At around 5.3 m occurs a disconformity that is followed by sediments bearing poorly preserved diatoms (*Denticulopsis hustedtii*, *Actinocyclus ingens*) that are probably middle to late Miocene in age. This is separated by another disconformity at around 3.4 m, from a section that was deposited in a time period around the Miocene/Pliocene boundary and the late early Pliocene. This can be deduced from the presence of *Cosmiodiscus intersectus*, *Denticulopsis hustedtii*, *Fragilariopsis arcula*, *F. praecurta* and *Thalassiosira convexa*, and the silicoflagellate *Distephanus speculum* f. *pseudofibula* (compare McCartney and Wise, 1990) in the lower part of

the section, followed by taxa indicative of the *Thalassiosira inura* and *Fragilariopsis barronii* zones. The foraminiferal ooze at the core top bears only trace diatoms. It can be assumed that its age falls in the late Pliocene to Quaternary time period (Fig. 8).

### 3.2. Gunnerus Ridge

During ANT-VIII/6 sediment cores were collected at six sites, all located on the northern part of the Gunnerus Ridge (Fig. 1, Table 1). Unfortunately, the sandy nature of the sediments on the surface of the Gunnerus Ridge prevented deep penetration at most sites. This resulted in four cores recovering less than 2 m and only one longer core, PS1812-6, with a length of 7.38 m. Coring attempts in the southern part of the Gunnerus Ridge failed due to non-penetration of the sediments.

The short cores PS1808-1, PS-1809-1, PS1810-1 and PS1820-6 (Table 1) contain diatomaceous and diatom-bearing sandy muds that are overlain by a 0.1–0.2 m thick veneer consisting of sandy silt that bears foraminifera. The diatomaceous sediment can be dated to late-mid Pliocene in age. In PS1820-6 the assemblages consist of a mixture of late Miocene to Pliocene diatoms, which indicates significant reworking. The calcareous layer at the top of the sediment column is separated by an erosive contact from the diatomaceous sequence.

Core PS1811-6 (core length 2.76 m, water depth 1147 m) consists of Pliocene diatom and diatom-bearing mud. The base of the core in in the early Pliocene *Fragilariopsis barronii* Zone, based on the occurrence of the nominate species accompanied by *Fragilariopsis praecurta*, *F. praeinterfrigidaria*, *F. reinholdii* and *Thalassiosira inura*. Around 1.6 m is the first occurrence of *Nitzschia interfrigidaria*, placing this interval just below the early/late Pliocene boundary. A disconformity at ca. 0.7 m separates this layer from sediments deposited during the time range of the *Thalassiosira insigna–T. vulnifica* Zone. This is topped by a 0.3 m-thick, foraminifer-bearing sandy silt, separated from the diatomaceous sediments by a disconformity.

Core PS1812-6 (core length 7.38 m, water depth 1356 m) consists of diatomaceous mud and diatom bearing sandy mud, topped by 0.8 m of sandy foraminiferal ooze ($\sim$50% carbonate content) and foraminiferal sandy mud (30% carbonate content) (Fig. 11). The base of the core is in the lowermost portion of the late Miocene *Actinocyclus ovalis* Zone as indicated by the co-occurrence of the nominate species and *Actinocyclus fryxellae*, *Denticulopsis hustedtii*, *Fragilariopsis arcula*, *F. praecurta*, *Thalassiosira gersondei* and *T. mahoodii*. This core section correlates with the time period between geomagnetic chrons C4n, C3Bn and C3An and thus documents sedimentation at ca. 0.2 cm per 1000 yr, between ca. 6.4 and 8.4 Ma. This interval is separated from early Pliocene sediments by a disconformity also indicated by a concentration of indurated pebbles that are cemented. The early Pliocene extends from the upper portion of the *Thalassiosira oestrupii* Zone to the lower part of the *Fragilariopsis interfrigidaria* Zone, deposited at an average sedimentation rate of 0.2 cm/1000 yr. Probably late Pliocene–Pleistocene sandy sediments containing foraminifera occur above another disconformity at 0.8 m.

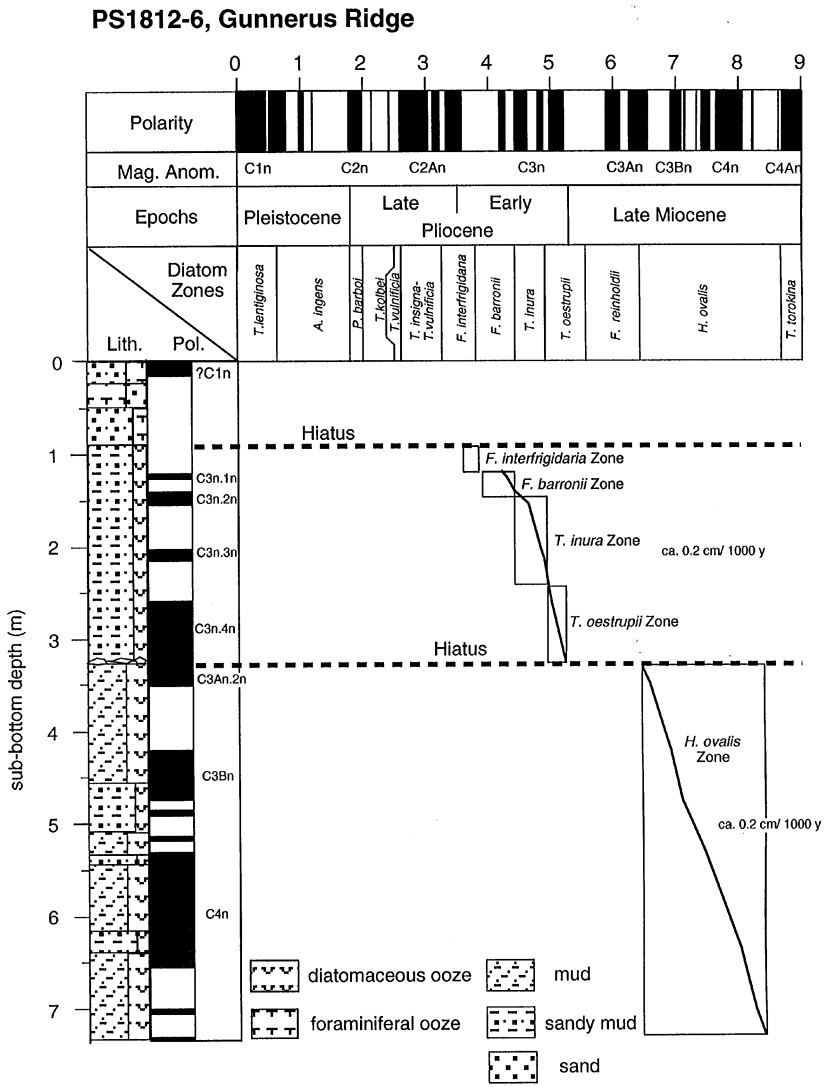


Fig. 11. Age-depth model for Core PS1812-6, based on combined diatom and geomagnetic polarity stratiography. Age assignment of geomagnetic polarities according to Cande and Kent (1995).

## 4. Discussion and summary

The geoscientific survey documents the sediment deposition on Gunnerus Ridge and the adjacent Kainan Maru Seamount (KMS). On KMS sediment deposits reaching a maximum thickness of ca. 200 m were examined by deep penetrating

Parasound-echosounding and additional sediment coring. Acoustically the sediments can be subdivided into well-layered sediment packages, separated by distinct reflectors named KM-A and KM-B, which represent discontinuities in the sediment record. The seismic reflectors and the surface topography show that the sediments of KMS are significantly affected by uneven sedimentation as well as by slumps and slides due to gravity-induced slope instability, which produce steep scarps.

The sediments between Reflectors KM-A and KM-B are on average 50 m thick at water depths above 1900 m and thicken to ca. 75 m in around 2100–2200 m of water (Fig. 4). Much stronger variations in sediment thickness occur above Reflector KM-B. From the summit region of KMS, where the package reaches up to 125 m in thickness, the sediments are rapidly thinned to only a few meters at water depths around 1900–2000 m (Figs. 4, 6 and 7). On deeper parts of the slope (down to 2300–2400 m), where the flank of the seamount drops rapidly to 5000 m, the thickness of the package above KM-B increases to ca. 75 m (Fig. 6), where it is not affected by sediment detachment. Considering the acoustic layering and the sediment ages from cores recovered at Scarp A and on the lower part of the seamount flank, which is not affected by slumping (Core PS1813-6, Fig. 6), it can be deduced that the sediments above KM-B are Neogene in age. However, a more or less complete Neogene section has been deposited only in the summit region of KMS. Below around 1700–1800 m water depths upper middle Miocene to early Pliocene sediments are not present, which leads to a reduction of this sediment package to predominantly early Miocene to middle middle Miocene sequences that are covered by a sequence of mid-Pliocene and Quaternary deposits (Fig. 8). The reduction in Miocene sediments is strongest at around 1900–2000 m water depths, where KM-B is overlain directly by the mid-Pliocene/Quaternary surface sediment layer. This pattern is probably related to changes in intermediate and deep water mass circulation and velocities that began around the Paleogene/Neogene boundary, when the Antarctic Circumpolar Current was established due to the separation of South America and the Antarctic Peninsula (Barker and Burrell, 1977).

At least three generations of slide and slump events were detected by the Parasound survey (Fig. 4). The unburied slide and slump event that affected the sediments above Reflector KM-B created the steep Scarp A, which allows sampling of early Oligocene to middle Miocene sediment sequences. The resulting slippage plane is covered by dislocated blocks of sediment. The slide event occurred around the early/late Pliocene boundary, because the steep scarp and the dislocated sediments on the slippage plane are covered by mid-Pliocene diatomaceous mud and Quaternary foraminiferal ooze, as seen in cores PS2591-1, PS2593-1, PS2594-1, PS2595-1 and PS1816-1 (Fig. 8). Reflector KM-B, which marks an earlier slump and slide event, was apparently sampled by the deepest core recovered at Scarp A (PS2595-1) and by Core 1816-1 recovered on the slippage plane below Scarp A. The age assignment of these cores indicates that KM-B has an age around the early/late Oligocene boundary (Fig. 8). This time period is marked by a rapid global sea level fall of around 150 m. The causes of this event are as yet unclear: there is no known significant event in the oxygen isotope curve (Barrett, 1994). No cores penetrated Reflector KM-A, which impedes dating of this event, which possibly also created scarps as recorded on PLKM-1 (Fig. 4). The

sediment instabilities at KMS might be linked to changes in water content in the biosiliceous sediment sequences, as well as to sediment facies alternations.

Possible triggers for slumping events might be changes in circulation pattern and sea level. Earthquakes could also be a trigger, as they are known to occur off the Antarctic Continent in the western Indian sector of the Southern Ocean (Kaminuma, 1995, Earthquake Information System, Center for Monitoring Research's experimental International Monitoring System).

The sediment coring allows the first insight to the types of sediment, their rates of sedimentation and changes in facies. The oldest sediments recovered are early Oligocene in age and are located between Reflectors KM-A and KM-B. Although in two cores these sediments contain biosiliceous components ranging between diatom-bearing muds and diatom ooze, only one (PS2595-1) recovered calcareous nannofossils in its lower portion. In contrast, Oligocene sequences recovered during ODP drilling at Maud Rise in water depths between 2100 and 2900 m are predominantly calcareous nannofossil ooze (Shipboard Scientific Party, 1988). The ODP sites 689 and 690 are located around 64°30′S and 65°S, respectively, thus at similar latitudes to KMS. This pattern is interesting, because it might indicate that early Oligocene water temperatures in the area of Kainan Maru Seamount were, at some time intervals, lower than in the Atlantic sector, preventing the production of calcareous nannofossils.

Considering an early Oligocene age for the interval below Reflector KM-B and a sediment thickness of at least 80 m below this reflector, as indicated by Parasound, it can be speculated that marine sedimentation started on KMS during the late Cretaceous.

Early Miocene and middle Miocene sediments were recovered at Scarp A and by Core PS1813-6, which penetrated sediments on the lower part of the KMS flank not affected by slumping. The sediments are diatom-bearing and diatomaceous mud in the early Miocene and predominantly diatom ooze in the middle Miocene. Sedimentation rates obtained from Core PS1813-6 are between 0.4 and 1.5 cm/1000 yr (Fig. 10). Late Miocene to mid-Pliocene sequences consist of diatom bearing and diatomaceous mud, both at Gunnerus Ridge and KMS. This accumulated at low sedimentation rates of a few milimeters per 1000 yr.

The mid-Pliocene diatomaceous mud and the Quaternary foraminiferal ooze are separated by a disconformity (Figs. 8–11). The same pattern and change in sedimentary facies from biosiliceous to foraminiferal sediments were also reported from Astrid Ridge (Gersonde in Fütterer et al., 1991) and Maud Rise (Abelmann et al., 1990) and thus represent a common feature in late Neogene-Quaternary sediment sequences deposited off the Antarctic Continent. Also the Lecointe Guyot (De Gerlache seamounts) in the Bellingshausen Sea (SE-Pacific sector) is covered by Quaternary foraminiferal ooze (Hagen et al., 1998). Abelmann et al. (1990) interpret the distinct change from biosiliceous to calcareous sedimentation to be related to a reorganization of water mass circulation triggered by the early late Pliocene increase of northern hemisphere ice sheet formation. As on Maud Rise and Astrid Ridge the sedimentation of the forminiferal sediments on KMS is at low rates that do not exceed 0.3–0.4 cm/1000 yr, as documented in PS1816-1 (Fig. 5). Gunnerus Ridge is covered by a veneer of

Quaternary foraminiferal deposits that were deposited at even lower rates. The carbonate consists mainly of *Neogloboquadrina pachyderma*. The sandy nature of the foraminiferal ooze prevented deep penetration of the coring device at some locations on KMS and at most locations on Gunnerus Ridge. It forms a prominent seismic bottom reflector (Figs. 4, 6, and 7).

The present study, combining bathymetric, sediment echosounding, and sediment coring data, provides the first more comprehensive overview of Cenozoic sedimentation in the remote area of the Gunnerus Ridge and Kainan Maru Seamount. The sediment record is affected by large scale slides and slumps and by probable current activities, which allow sampling of the Cenozoic sediment record using conventional coring. The Parasound survey and sediment coring achieved during RV "Polarstern" cruises ANT-VIII/6 and ANT-XI/4 provides a baseline for further sediment coring with conventional piston corers to collect a more complete section of the Cenozoic sediments in this area. This would increase our knowledge of the Cenozoic evolution of the Antarctic cryosphere, based on sampling techniques that are compared relatively low cost with deep-sea drilling.

## Acknowledgements

We kindly thank John Barron and an anonymous reviewer for constructive review and comments. We also acknowledge the technical assistance of U. Bock. This work was generously supported by the Deutsche Forschungsgemeinschaft and Acciones Integradas. This is Alfred Wegener Contribution No. 1345.

## References

Abelmann, A., Gersonde, R., Spiess, V., 1990. Pliocene–Pleistocene paleoceanography in the Weddell Sea – siliceous Microfossil evidence. In: Bleil, U., Thiede, J. (Eds.), Geological History of the Polar Oceans: Arctic Versus Antarctic, Nato-ASI Series C: Mathematical and Physical Science, Vol. 308, 729–759.

Akiba, F., Yanagisawa, Y., 1986. Taxonomy, morphology and phylogeny of the Neogene diatom zonal markers species in the middle-to-high latitudes of the North Pacific. In: Kamagi, H., Karig, D.E., Coulbourn, W.T., et al. (Eds.), Initial Reports of the Deep Sea Drilling Project, Vol. 87. U.S. Government Printing Office, Washington D.C., pp. 483–554.

Baldauf, J.G., Barron, J.A., 1991. Diatom biostratigraphy: Kerguelen Plateau and Prydz Bay regions of the Southern Ocean. In: Barron, J., Larsen, B., et al. (Eds.), Proceedings of the Ocean Drilling Program, Scientific Results, Vol. 119, Ocean Drilling Progam, College Station, Texas, pp. 547–598.

Barker, P.F., Burrell, J., 1977. The opening of Drake Passage. Marine Geology 25, 15–34.

Barker, P.F., Kennett, J.P., et al., 1988. Proceedings of the Ocean Drilling Program, Initial Reports, vol. 113, 785 p. Ocean Drilling Program, College Station, Texas.

Barrett, P.J., 1994. Progress towards a Cenozoic Antarctic glacial history. Terra Antarctica 1, 247–248.

Barron, J.A., Mahood, A.D., 1993. Exceptionally well-preserved early Oligocene diatoms from glacial sediments of Prydz Bay, East Antarctica. Micropaleontology 39, 29–45.

Berggren, W.A., Kent, D.V., Swisher, C.C., Aubry, M.P. 1995. A revised Cenozoic Geochronology and Chonostratigraphy. In: Berggren, W.A. et al. (Eds.), Geochronology Time Scales and Global Stratigraphic Correlation, SEPM, Special Publ. No. 54, 129–212.

Cande, S.C., Kent, D.V., 1995. Revised calibration of the geomagnetic polarity timescale for the Late Cretaceous and Cenozoic. Journal of Geophysical Research 100, 6093–6095.

Ciesielski, P.F., 1983. The Neogene and Quaternary diatom biostratigraphy of Subantarctic sediments, Deep Sea Drilling Project Leg 71. In: Ludwig W.J., Krasheninnikov, V.A., et al. (Eds.), Initial Reports of the Deep Sea Drilling Project, vol. 71(2). U.S. Government Printing Office, Washington, D.C. pp. 635–665.

Ciesielski, P.F., 1986. Middle Miocene to Quaternary diatom biostratigraphy of the Deep Sea Drilling Project Site 594, Chatham Rise, southwest Pacific. In: Kennett, J.P., von der Borch, C.C., et al. (Eds.), Initial Reports of the Deep Sea Drilling Project, Vol. 90. U.S. Government Printing Office, Washington, D.C., pp. 863–885.

Fenner, J., 1978. Cenozoic diatom biostratigraphy of the equatorial and southern Atlantic Ocean. In: Supko, P.R., Perch-Nielsen, K., et al. (Eds.), Initial Reports of the Deep Sea Drilling Project, Vol. 39 (Suppl.), U.S. Government Printing Office, Washington, D.C. pp. 491–623.

Fenner, J., 1984a. Eocene-Oligocene planktic diatom stratigraphy in the low and high southern latitudes. Micropaleontology 30, 319–342.

Fenner, J., 1984b. Middle Eocene to Oligocene planktonic diatom stratigraphy from Deep Sea Drilling sites in the south Atlantic, equatorial Pacific and Indian Ocean. In: Hay, W.W., Sibuet, J.-C., et al. (Eds.), Initial Reports of the Deep Sea Drilling Project, vol. 75 (Part. 2), U.S. Government Printing Office, Washington D.C., pp. 1245–1271.

Fenner, J., 1985. Late Cretaceous to Oligocene planktic diatoms. In: Bolli, H.M., Saunders, J.B., Perch-Nielsen, K. (Eds.), Plankton Stratigraphy, vol. 2, pp. 713–762.

Fütterer, D.K., Schrems, O., et al., 1991. The expedition ANTARKTIS-VIII of RV "Polarstern" 1989/1990, Reports of Legs ANT-VII/6-7. Reports on Polar Research vol. 90, 231 p.

Gersonde, R., 1990. Taxonomy and morphostructure of Neogene diatoms from the Southern Ocean, ODP Leg 113. In: Barker, P.F., Kennett, J.P., et al. (Eds.), Proceedings of the Ocean Drilling Program, vol. 113, Scientific Results, Ocean Drilling Program, College Station, Texas, pp. 791–802.

Gersonde, R., 1991. Taxonomy of morphostructure of late Neogene Diatoms from Maud Rise (Antarctic Ocean). Polarforschung 59(3), 141–171.

Gersonde, R., Burckle, L.H., 1990. Neogene diatom biostratigraphy of ODP Leg 113, Weddell Sea (Antarctic Ocean). In: Barker, P.F., Kennett, J.P., et al. (Eds.), Proceedings of the Ocean Drilling Program, Scientific Results, vol. 113, Ocean Drilling Program, College Station, Texas, pp. 761–789.

Gersonde, R., Bárcena, M.A., 1998. Revision of the late Pliocene–Pleistocene diatom biostratigraphy for the northern belt of the Southern Ocean. Micropaleontology 44(1), 84–98.

Gladenkov, A.Y., Barron, J.A., 1995. Oligocene and early middle Miocene diatom biostratigraphy of Hole 884B. In: Rea, D.K., Basov, I.A., Scholl, D.W., Allan, J. F., (Eds.), Proceedings of the Ocean Drilling Program, Scientific Results, vol. 145, Ocean Drilling Program, College Station, Texas pp. 21–41.

Gombos, A.M., 1977. Paleogene and Neogene diatoms from the Falkland Plateau and Malvinas outer basin, Leg 36. Deep Sea Drilling Project. In: Barker, P.F., Dalziel, I.W.D., et al. (Eds.), Initial Reports of Deep Sea Drilling Project, vol. 36, U.S. Government Printing Office, Washington, pp. 575–687.

Gombos, A.M., 1983. Middle Eocene diatoms from the South Atlantic. In: Ludwig, W.J., Krasheninikov, V.A., et al. (Eds.), Initial Reports of Deep Sea Drilling Projects, vol. 36, U.S. Government Printing Office, Washington, pp. 565–581.

Gombos, A.M., Ciesielski, P.F., 1983. Late Eocene to early Miocene diatoms from the southwest Atlantic. In: Ludwig, W.J., Krasheninikov, V.A., et al. (Eds.), Initial Reports of Deep Sea Drilling Project, vol. 71, U.S. Government Printing Office, Washington. pp. 583–634.

Gutberlet, M., Schenke, H.-W., 1989. Hydrosweep: New era in high precision bathymetric surveying in deep and shallow water. Marine Geodesy 13, 1–23.

Hagen, R.A., Gohl, K., Gersonde, R., Kuhn, G., Völker, D., Kodagali, V.N., 1998. A geophysical study of the De Gerlache Seamounts: preliminary results. Geo-Marine Letters 18, 19–25.

Harwood, D.M., 1986. Diatoms. In: Barrett, P.J. (Ed.), Antarctic Cenozoic History from the CIROS-1 Drillhole, McMurdo Sound, DSIR Bulletin, N.Z., vol. 237, pp. 69–107.

Harwood, D.M., 1989. Siliceous microfossils. In: Barrett, P.J. (Ed.), Antarctic Cenozoic History from the MSSTS-1 Drillhole, McMurdo Sound, DSIR Bulletin, N.Z. Vol. 245, pp. 67–97.

Harwood, D.M., Maruyama, T., 1992. Middle Eocene to Pleistocene diatom biostratigraphy of Southern Ocean sediments from the Kerguelen Plateau, Leg 120. In: Wise Jr., S.W., Schlich, R., et al. (Eds.), Proceedings of the Ocean Drilling Program, Scientific Results, vol. 120. Ocean Drilling Program, College Station, Texas, pp. 683–733.

Kaminuma, K., 1995. Seismicity around the Antarctic Peninsula. Proceedings of the NIPR Symposium on Antarctic Geoscience, 8, 25–42.

McCartney, K., Wise Jr., S.W., 1990. Cenozoic silicoflagellates and ebridians from ODP Leg 113: Biostratigraphy and notes on morphologic variability. In: Barker, P.F., Kennett, J.P., et al. (Eds.), Proceeding of the Ocean Drilling Ocean, Scientific Results, vol. 113, Ocean Drilling Program, College Station, Texas, pp. 729–760.

Perch-Nielsen, K., 1985a. Cenozoic calcareous nannofossils. In: Bolli, H.M., Saunders, J.B., Perch-Nielsen, K., (Eds.), Plankton stratigraphy, vol. 1, pp. 427–554.

Perch-Nielsen, K., 1985b. Silicoflagellates, In: Bolli, H.M., Saunders, J.B., Perch-Nielsen, K., (Eds.), Plankton Stratigraphy, vol. 2, pp. 811–846.

Roeser, H.A., Fritsch, J., Hinz, K., 1996. The development of the crust off Dronning Maud Land, East Antarctica. In: Storey, B.C., King, E.C., Livermore, R.A. (Eds.), Wedell Sea Tectonics and Gondwana Break-up, Geological Society Special Publication, vol. 108, pp. 243–264.

Saki, T., Tamura, Y., Tokuhashi, S., Kodato, T., Mizukoshi, I., Amano, H., 1987. Preliminary report of geological and geophysical surveys off Queen Maud Land, east Antarctica. Proceedings of NIPR Symposium Antarctic Geoscience, vol. 1, pp. 23–40.

Schrader, H.J., 1973. Cenozoic diatoms from the northeast Pacific, Leg 18. In: Kulm, L.D., von Huene, R., et al. (Eds.), Initial Reports of the Deep Sea Drilling Project, vol. 18. U.S. Government Printing Office, Washington, D.C., pp. 673–797.

Schrader, H.-J., 1976. Cenozoic marine planktonic diatom biostratigraphy of the Southern Pacific Ocean. In: Hollister, C.D., Craddock, C., et al. (Eds.), Initial Reports of the Deep Sea Drilling Project, vol. 35, U.S. Government Printing Office, Washington, D.C., pp. 605–671.

Schrader, H.-J., Fenner, J., 1976. Norwegian Sea Cenozoic diatom biostratigraphy and taxonomy, In: Talwani, M., Udintsev, G., et al. (Eds.), Initial Reports of the Deep Sea Drilling Project, vol. 38, U.S. Government Printing Office, Washington, D.C., pp. 921–1089.

Sheshukova-Poretzkaya, V.S., 1962. New and rare Bacillariophyta from diatom series of Sakhalin Island. Uch. Zap. Igu. Ser. Biol. Nauk (Leningrad Univ.), 49, 203–211.

Shipboard Scientific Party, 1988. Sites 689 and 690. In: Barker, Kennett, J.P., et al. (Eds.), Proceedings of the Ocean Drilling Program, Initial Reports, vol. 113, Ocean Drilling Program, College Station, Texas, pp. 89–292.

Wei, W., Wise, S.W. Jr., 1990. Middle Eocene to Pleistocene calcareous nannofossils recovered by Ocean Drilling Program Leg 113 in the Weddell Sea. In: Barker, P.F., Kennett, J.P., et al. (Eds.), Proceedings of the Ocean Drilling Program, Scientific Results, vol. 113, Ocean Drilling Program, College Station, Texas, pp. 639–666.

Wei, W., Wise, S.W., 1992. Selected Neogene calcareous nannofossil index of the Southern Ocean: Biochronology, Biometrics, and Paleoceanography. In: Wise, S.W., Jr., Schlich, R., et al. (Eds.), Proceedings of the Ocean Drilling Program, Scientific Results, vol. 120. Ocean Drilling Program, College Station, Texas, pp. 523–537.

Wise, S.W. Jr., 1983. Mesozoic and Cenozoic calcareous nannofossils recovered by Deep Sea Drilling Project Leg 71 in the Falkland Plateau region. Southwest Atlantic Ocean. In: Ludwig, W.J., Krasheninnikov, V.A., et al. (Eds.), Init. repts. DSDP, vol. 71. U.S. Government Printing Office, Washington, pp. 481–550.

Yanakisawa, Y., Akiba, F., 1990. Taxonomy and phylogeny of the three marine diatom genera, Crucidenticula, Denticulopsis and Neodenticula. Bulletin of the Geological Survey of Japan 41, 197–301.

Young, J.R., Flores, J.A., Wei, W., 1994. A summary chart of Neogene Nannofossil magnetobiostratigraphy. Journal of Nannoplankton Research 16(1), 21–27.